

Thermal neutron shielding performance and mechanism of a novel, low cost material: Boron-rich slag

Mengge Dong^a, Xiangxin Xue^{a, *}

^a Department of Resource and Environment, School of Metallurgy, Northeastern University, Shenyang 110004, China;

Corresponding author: xuexx@mail.neu.edu.cn (Xiangxin Xue)

Abstract: In this paper, thermal shielding performance and mechanism of boron-rich slag was studied. Data of neutron scattering lengths and cross sections were used to analyze the shielding properties and mechanism. It was found that the macro-cross section of boron-rich slag is 5.02 cm^{-1} , higher than ordinary concrete, PE-B₄C concrete, FeCr slag and colemanite concentrator for neutron shielding. The maximum contribution of the elements contained in boron-rich slag for shielding thermal neutron was B, it was 92.85%, far more than the contribution of other elements. $2\text{MgO}\cdot\text{B}_2\text{O}_3$ was the main compound of boron-rich slag for shielding thermal neutron. Main shielding forms are elastic and absorption. However, the effect of absorption was far more than elastic. Besides, the effect of absorption emitted the gamma ray was the biggest. Boron-rich slag would be excellent shielding material or filler for neutron shielding. Besides, the investigation provides a method to analyze the shielding mechanism of complex shielding material for thermal neutron.

Key words: boron-rich slag; thermal neutron; shielding properties; mechanism

1 Introduction

Boron reserve of China ranks fourth in the world next to Turkey, USA and Russia. In China, the main boron-containing ores are szaibelyite, ludwigite and brine. However, Ludwigite resource is relatively abundant and account for 58.4% of the total Chinese boron reserve [1]. The main utilization method for Ludwigite is used to produce pig iron. Besides, iron slag would be emitted which is named as boron-rich slag, moreover, the slag is mainly used for the production of boron products [1-3]. It is well known that boron has excellent shielding property for neutron radiation protection. For example, B₄C/ Al composites were successfully fabricated by vacuum hot pressing followed by hot rolling in atmospheric environments for shielding thermal neutron, it was found the materials has good properties [4]; Khong *et al* [5] investigated some new alloys contained boron for neutron shielding. In addition, Li *et al* [6-8] had used the boron-rich slag to make composites with epoxy resin matrix for shielding thermal neutron, it was found the shielding properties were excellent. However, the shielding properties of boron-rich slag itself for thermal neutron have never been studied. Moreover, the shielding mechanism for thermal had not been studied.

Neutron scattering lengths and cross sections of the elements and their isotopes for thermal neutron ($E= 25.3\text{meV}$, $V= 2200 \text{ m/s}$) was reported by Sears [9]. Besides, the data was widely used in many studies [10-21]. For example, Leguy *et al* [10] used the data to analyze scattering cross-section of H in their research. Hillborg *et al* [13] calculated the coherent scattering length of some polymers using the data. Özdemir *et al* [20, 21] investigated the shielding performance of some boron containing materials for shielding thermal neutron using the data. Besides, the past studies had not investigated the shielding mechanism for thermal neutron; this encourages us to do this investigation.

In this work, shielding properties and mechanism of boron-rich slag for thermal neutron shielding will be studied. The investigation will provide useful utilization information for boron-rich slag in the field of shielding material application and a method to analyze the shielding mechanism of complex shielding material for thermal neutron.

2 Material and methods

2.1 Material

The raw material used in the work was boron-rich slag (Density=2.97 g/cm³, Fengcheng Iron and Steel Group Co. Ltd. of Dandong). Table 1 shows the chemical composition of boron-rich slag, besides, the content of B-10 and B-11 is calculated according to the abundance of B-10 and B-11 contained in

natural boron [5]. Fig.1 shows the SEM of boron-rich slag and distribution of boron element contained in the raw material. Fig.2 shows the XRD pattern of boron-rich slag, it is found that the main compounds of boron-rich slag are $2\text{MgO}\cdot\text{B}_2\text{O}_3$, Mg_2SiO_4 and Ca_2SiO_4 .

Table 1 Chemical composition of boron-rich slag (wt%)

Element	B	O	C	Mg	Al	Si	Ca	Fe
Boron-rich slag	3.65	42.097	7.364	21.068	3.727	10.763	10.541	0.79

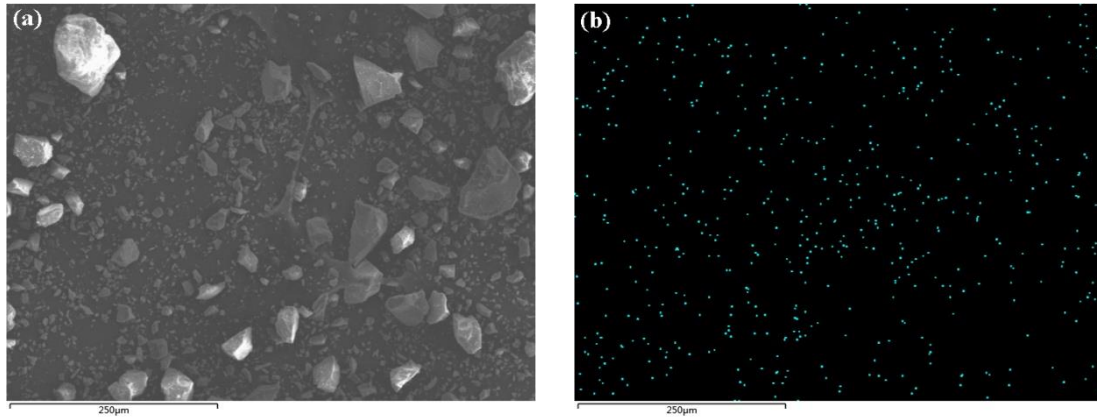


Fig.1. SEM of boron-rich slag (a) and distribution of boron element (b)

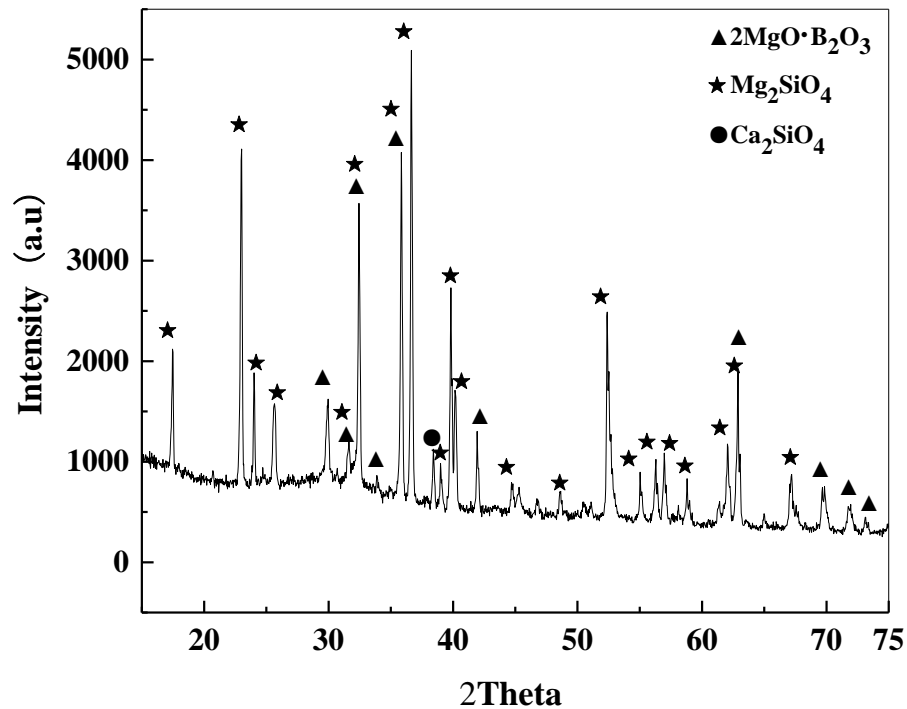


Fig.2. XRD pattern of boron-rich slag

2.2 Methods

It is well known that Sears reported the neutron scattering lengths and cross sections which provided the bound coherent scattering cross section, bound incoherent scattering cross section and

absorption cross section of the elements and their isotopes for thermal neutron [9], while the energy of thermal neutron was 25.30meV [9, 20, 21]. Besides, the total micro cross section could be calculated as follows:

$$\sigma = \sigma_1 + \sigma_2 + \sigma_3 \quad (1)$$

Where σ is total micro cross section, σ_1 is the bound coherent scattering cross section, σ_2 is the bound incoherent scattering cross section and σ_3 is absorption cross section. Table 2 shows the total micro cross section of the elements contained in boron-rich slag from the data reported by Sears [9].

Table 2 Micro cross section of elements contained in boron-rich slag for thermal neutron

Element	B	O	C	Mg	Al	Si	Ca	Fe
Micro-cross section (barn)	772.24	4.23219	5.5545	3.773	1.734	2.338	3.26	14.18

While the macro cross section of boron-rich slag (ΣE , cm^{-1}) could be calculated as follows [8, 22]:

$$\Sigma E = N_A \rho \sum_i \frac{\omega_i}{M_i} (\sigma)_i \quad (2)$$

$$\Sigma E = \sum_i \omega_i (\Sigma E)_i \quad (3)$$

Where ΣE (cm^{-1}) is the macro-cross section of boron-rich slag, ω_i is the mass fraction of i th element, N_A is the Avogadro Constant, ρ (g/cm^3) is the density of boron-rich slag, M_i is the molar mass of i th element, $(\sigma)_i$ (measured in barn) is micro-cross section of i th element.

Thus the contribution of each element contained for the macro cross section of boron-rich slag could be calculated as follows:

$$C = \frac{N_A \rho \frac{\omega_i}{M_i} (\sigma)_i}{\Sigma E} \times 100\% \quad (3)$$

3 Results and discussion

3.1 Shielding properties of boron-rich slag for thermal neutron

It can be seen from the Table 2 that the maximum micro-cross section is B, next is Fe, and other elements are nearly the same. Besides, the value of micro-cross section of B is far more than other elements. The result of the macro-cross section of boron-rich slag is 5.02 cm^{-1} . Fig. 3 shows the comparative of boron-rich slag and some concretes and fillers for neutron shielding, it is found that the macro cross section of boron-rich slag is higher than ordinary concrete, PE-B4C concrete, FeCr slag and colemanite concentrator for neutron shielding. It can be that the boron-rich slag would be excellent

shielding material or filler for neutron shielding.

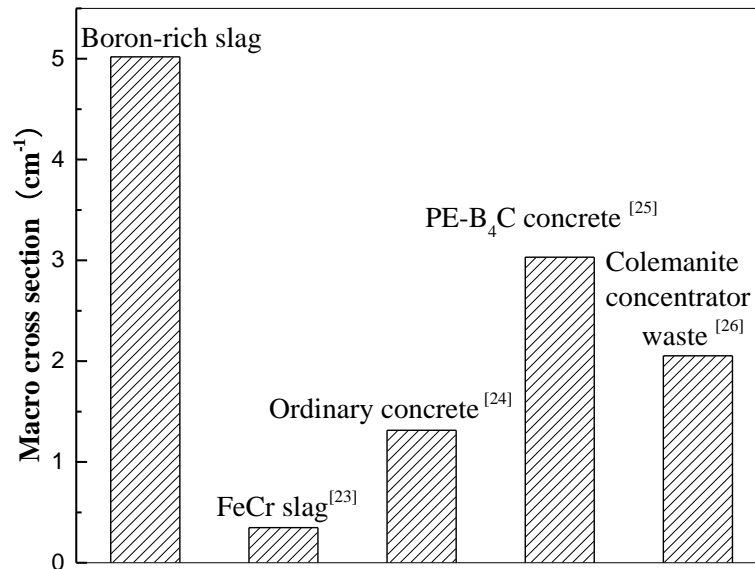


Fig.3. Macro cross section of some concretes and fillers for neutron shielding

3.2 Shielding mechanism of boron-rich slag for thermal neutron

Table 3 Contribution of each element contained in boron-rich slag for thermal neutron shielding

Element	B	O	C	Mg	Al	Si	Ca	Fe
Contribution(%)	92.85	3.97	1.26	1.15	0.09	0.32	0.31	0.07

The contribution of each element contained in boron-rich slag for thermal neutron shielding is shown in Table 3. From Table3, it can be seen that the maximum contribution of the elements contained in boron-rich slag is B, it is 92.85%, far more than the contribution of other elements. Next is O (3.97%), C(1.26%), Mg(1.15%), however, the contribution of Al, Si, Ca and Fe is relatively samll. Combined with XRD pattern of boron-rich slag (Fig.2), it is found that the main compounds of boron-rich slag are $2MgO \cdot B_2O_3$, Mg_2SiO_4 and Ca_2SiO_4 , besides, the $2MgO \cdot B_2O_3$ is the only compound contains the boron element in the slag. Nevertheless, Mg_2SiO_4 contains little Mg and O. Thus $2MgO \cdot B_2O_3$ is the main compound for shielding thermal neutron and far more than other compounds. Thus, the shielding mechanism of boron-rich slag for thermal neutron can be concluded as shown in Fig.4. It can be seen that the main shielding forms are elastic and absorption. However, the effect of absorption is far more than elastic. Besides, the effect of absorption emitted the gamma ray is the biggest [27-29].

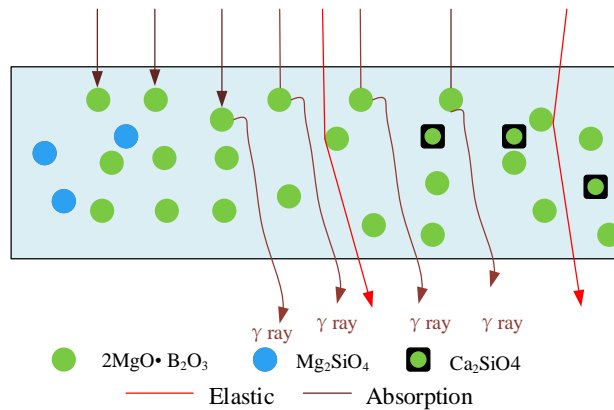


Fig.4. Shielding mechanism of boron-rich slag for shielding thermal neutron

4 Conclusions

The result of the macro-cross section of boron-rich slag is 5.02 cm^{-1} , higher than ordinary concrete, PE-B₄C concrete, FeCr slag and colemanite concentrator for neutron shielding.

The maximum contribution of the elements contained in boron-rich slag for shielding thermal neutron is B, it is 92.85%, far more than the contribution of other elements. 2MgO·B₂O₃ is the main compound of boron-rich slag for shielding thermal neutron. Main shielding forms are elastic and absorption. However, the effect of absorption is far more than elastic. Besides, the effect of absorption emitted the gamma ray is the biggest.

Boron-rich slag would be excellent shielding material or filler for neutron shielding. Besides, the investigation provides a method to analyze the shielding mechanism of complex shielding material for thermal neutron.

Acknowledgements

This work was supported by National Natural Science Foundation of China (51472048 and 50774022) and The Key Laboratory Project of Liaoning Province Education Office (LZ 2014-022).

References

- [1] An, J., Xue, X.X.: Life cycle environmental impact assessment of borax and boric acid production in China. *J. Clean. Prod.* 66, 121–127 (2014)
- [2] Jiang, T., Wu, J.B., Xue, X.X., Duan, P.N., Chu, M.S.: Carbothermal formation and microstructural evolution of α' -Sialon-AlN-BN powders from boron-rich blast furnace slag. *Adv. Powder Technol.* 23, 406–413 (2012)
- [3] Wang, G., Xu, Q.G., Wang, J.S.: Effect of Na₂CO₃ on reduction and melting separation of

- ludwigite /coal composite pellet and property of boron-rich slag. *T. Nonferr. Metal. Soc.* 26, 282–293 (2016)
- [4] Chen, H.S., Wang, W.X., Li, Y.L., Zhang, P., Nie, H.H., Wu, Q.C.: The design, microstructure and tensile properties of B₄C particulate reinforced 6061Al neutron absorber composites. *J. Alloy. Compd.* 632, 23–29 (2015)
- [5] Khong, J. C., Daisenberger, D., Burca, G., Kockelmann, W., Tremsin, A. S., Mi, J.: Design and Characterisation of Metallic Glassy Alloys of High Neutron Shielding Capability. *Sci. Rep-UK.* 36998 (2016)
- [6] Li, Z.F., Xue, X.X., Jiang, T., Yang, H., Zhou, M.: Study on the properties of boron containing ores/Epoxy composites for slow neutron shielding. *Adv. Mater. Res.* 201–203, 2767–2771 (2011)
- [7] Li, Z.F., Xue, X.X., Duan, P.N., Tian, A., Li, S.X., Yin, Z.S.: Preparation and thermal/fast neutron shielding properties of novel boron containing ore composites. *Mater. Sci. Forum.* 743–744, 613–622 (2013)
- [8] Li, Z.F., Xue, X.X., Liu, S.L., Li, Y., Duan, P.N.: Effects of boron number per unit volume on the shielding properties of composites made with boron ores from China. *Nucl. Sci. Tech.* 23, 344–348 (2012)
- [9] Sears, V. F.: Neutron Scattering Lengths and Cross Sections. *Neutron News.* 3, 29–37 (1992)
- [10] Leguy, A. M. A., Frost, J. M., McMahon, A. P., Sakai, V. G., Kockelmann, W., Law, C. H., Li, X., Foglia, F., Walsh, A., O'Regan, B. C., Nelson, J., Cabral, J. T., Barnes, P. R. F.: The dynamics of methylammonium ions in hybrid organic-inorganic perovskite solar cells. *Nat. Commun.* 6, 7124 (2015)
- [11] Bruni, F., Imberti, S., Mancinelli, R., Ricci, M. A.: Aqueous solutions of divalent chlorides: ions hydration shell and water structure. *J. Chem. Phys.* 136, 064520 (2012)
- [12] Allen, A. J., Thomas, J. J., Jennings H. M.: Composition and density of nanoscale calcium-silicate-hydrate in cement. *Nat. Mater.* 6, 311 (2007)
- [13] Hillborg, H., Ankner, J. F., Gedde, U. W., Smith, G. D., Yasuda, H. K., Wikström, K.: Crosslinked polydimethylsiloxane exposed to oxygen plasma studied by neutron reflectometry and other surface specific techniques. *Polymer.* 41, 6851–6863 (2000)
- [14] And, T. J. S., Lu, J. R., Thomas, R. k., Cui, Z. F., Penfold J.: The Effect of Solution pH on the Structure of Lysozyme Layers Adsorbed at the Silica-Water Interface Studied by neutron

- reflection. *Langmuir*. 14, 438–445 (1998)
- [15] Mancinelli, R., Botti, A., Bruni, F., Ricci, M. A., Soper, A. K.: Hydration of sodium, potassium, and chloride ions in solution and the concept of structure maker/breaker. *J. Phys. Chem. B*. 111, 13570–7 (2007)
- [16] Piscitelli, F., Van, E. P.: Analytical modeling of thin film neutron converters and its application to thermal neutron gas detectors. *J. Instrum.* 8, 174–174 (2013)
- [17] MacDonald, J. C., Dorrestein, P. C., Pilley, M. M., Foote, M. M., Lundburg, J. L., Henning, R. W., Schultz, A. J., Manson J. L.: Design of Layered Crystalline Materials Using Coordination Chemistry and Hydrogen Bonds. *J. Am. Chem. Soc.* 122, 11692–11702 (2015)
- [18] Zeidler, A., Wezka, K., Rowlands, R. F., Whittaker, D. A., Salmon, P. S., Polidori, A., Drewitt, S., Klotz, J. W., Fischer, H. E., Wilding, M. C., Bull, C. L., Tucker, M. G., Wilson, M.: High-pressure transformation of SiO₂ glass from a tetrahedral to an octahedral network: a joint approach using neutron diffraction and molecular dynamics. *Phys. Rev. Lett.* 11350, 5762–5770 (2014)
- [19] Bolisetty, S., Vallooran, J. J., Adamcik, J., Mezzenga, R.: Magnetic-Responsive Hybrids of Fe₃O₄ Nanoparticles with beta-Lactoglobulin Amyloid Fibrils and Nanoclusters. *Acs Nano*. 7, 6146 (2013)
- [20] Özdemir, T., Akbay, İ.K., Uzun, H., Reyhancan İ.A.: Neutron shielding of EPDM rubber with boric acid: Mechanical, thermal properties and neutron absorption tests. *Prog. Nucl. Energ.* 89, 102–109 (2016)
- [21] Özdemir, T., Güngör, A., Reyhancan, İ.A.: Flexible neutron shielding composite material of EPDM rubber with boron trioxide: Mechanical, thermal investigations and neutron shielding tests. *Radiat. Phys. Chem.* 131, 7–12 (2017)
- [22] Dong, M., Xue, X., Singh, V. P., Yang, H., Li, Z., Sayyed, M. I.: Shielding effectiveness of boron-containing ores in Liaoning province of China against gamma rays and thermal neutrons. *Nucl. Sci. Tech.* (2018). doi: 10.1007/s41365-018-0397-x
- [23] Korkut, T., Çay, V. V., Sütçü, M., Gencel, O.: Neutron radiation tests about Fe-Cr slag and natural zeolite loaded brick samples. *Sci. Technol. Nucl. Ins.* 2014, 190–193 (2014)
- [24] Bashter, I.I.: Calculation of radiation attenuation coefficients for shielding concretes. *Ann. Nucl. Energy*. 24, 1389–1401 (1997)
- [25] Demir, D., Keleş, G.: Radiation transmission of concrete including boron waste for 59.54 and

- 80.99 keV gamma rays. Nucl. Instru. Meth. B. 245, 501–504 (2006)
- [26] DiJulioa, D. D., Cooper-Jensena, C. P., Perreya, H., Fissuma, K., Rofors, E., Scherzingera, J., Bentleya, P. M.: A polyethylene-B₄C based concrete for enhanced neutron shielding at neutron research facilities. Nucl. Instru. Meth. A. 859, 41–46 (2017)
- [27] Chadwick, M.B., Herman, M., Obložinský, P., Dunn, M.E., Danon, Y., et al.: ENDF/B-VII.1 Nuclear Data for Science and Technology: Cross Sections, Covariances, Fission Product Yields and Decay Data. Nucl. Data. Sheets. 112, 2887–2996 (2011)
- [28] Ilas, G., Gauld, I.C., Radulescu, G.: Validation of new depletion capabilities and ENDF/B-VII data libraries in Scale. Ann. Nucl. Energy. 46, 43–55 (2012)
- [29] Ninyong, K., Wimolmala, E., Sombatsompop, N., Saenboonruang, K.: Potential use of NR and wood/NR composites as thermal neutron shielding materials. Polym. Test. 59, 336–343 (2017)